

南京航空航天大学
论文集

(二〇〇〇年)

第5册

一院

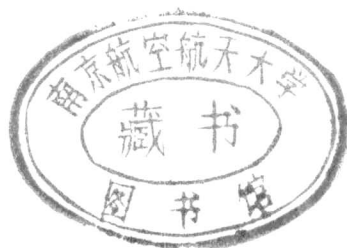
南京航空航天大学科技部编

二〇〇一年六月

h2471

— 院

○一三系(二)~○一四系



目 录

序号	姓名	职称	单位	论文题目	刊物、会议名称	年、卷、期	类别
105	陈 勇 陶宝祺	讲师	013	复合材料层板构件气弹振动控制实验研究	实验力学	001504	J
106	陈 勇	讲师	013	Analysis of an electrostrictive stack actuator for active trailing edge flaps	Chinese Journal of Aeronautics	001304	H
107	梁大开 邱 浩 陶宝祺	副教授	013	碳敷层光纤在碳纤维复合材料智能结构中的应用	南京航空航天大学学报	003206	J
108	梁大开 陶宝祺 朱晓荣	副教授	013	光纤智能复合材料结构的研究	仪器仪表学报	992006	H*
109	梁大开 黄明双 陶宝祺	副教授	013	光纤埋入碳纤维复合材料结构的实验研究	材料工程	000002	H
110	邱 浩 温卫东 梁大开 杨 红	硕士	013	一种用于复合材料固化监测的传感器的研究	光纤与电缆及应用技术	000006	J
111	邱 浩 温卫东 梁大开 杨 红 陶宝祺	硕士	013	复合材料固化监测用的光纤表面等离子体波传感器的研究	中国航空学会第十届航空发动机结构强度与振动会议	2000	
112	黄明双 梁大开 邱 浩 陶宝祺	博士后	013	Development of extrinsic fabry-Perot fiber sensor and its application to cmact materials	南京航空航天大学学报	001701	J
113	骆 英 陶宝祺	博士	013	1-3 型 OPCM 传感元件测量 OM 结构表面动态应力研究	应用力学学报	001704	J*
114	骆 英 熊 克 陶宝祺	博士	013	具有正交异性的压电复合材料力学量传感器的研究	中国力学 2000 年学术会议	2000	
115	骆 英 陶宝祺	博士	013	1-3 型 OPCM 应变传感元件的传感机理的研究	力学与实践	002206	H*
116	骆 英 陶宝祺	博士	013	土木工程智能结构中传感器原理与应用	江苏理工大学学报	002105	J*
117	骆 英 陶宝祺	博士	013	Research on Orthotropic Piezoelectric Composite Material Strain Sensing Units	Proceedings of SPIE	2000	
118	骆 英 张志华 陶宝祺	博士	013	混合编程及其在力学计算中的应用	计算机应用研究	000005	J*
119	骆 英 陶宝祺	博士	013	The Opcm Strain Gauges for Strain & Stress Measurement of the orthotropic Material Structures	Acta Mechanical Sinica	001304	
120	徐红星 骆 英 陶宝祺	硕士	013	关于 PZT 驱动性能的研究	中国力学 2000 年学术会议	2000	

序号	姓名	职称	单位	论文题目	刊物、会议名称	年、卷、期	类别
121	黄 睿 袁慎芳 陶宝祺	博士	013	Application of Optic Fiber Sensors Embedded onto Braided Composites	Proceedings of SPIE	2000	
122	袁慎芳 黄 睿 谢蒙萌 陶宝祺	副教授	013	Experimental Study on Optic Performance of Optic Fiber Braided in Carbon Fiber Braided Composites	南京航空航天大学学报 (英文版)	001702	J
123	袁慎芳 黄 睿 谢蒙萌 陶宝祺	副教授	013	Research on Optic Performances of Optic Fiber Braided in Carbon Fiber Braided Composites	南京航空航天大学学报 (英文版)	001702	J
124	袁慎芳 陶宝祺 石立华	副教授	013	一种飞机结构结冰监测及自适应除冰的模拟试验	航空学报	002106	H
125	袁慎芳 朱晓荣	副教授	013	应用应力波技术的蜂窝结构损伤监测	数据采集与处理	001504	H
126	吕益艳 王帮峰 吴安德 黄因慧		013	发展中的电铸技术	电加工与模具	000004	
127	王帮峰 张瑞芳	博士后	013	液压起升机构的非线性动力学研究	起重运输机械	000010	J
128	王帮峰	博士后	013	回转起重机吊重摆振的机器人动力学模型	南京航空航天大学学报 (英文版)	001701	J
129	刘福强 张令弥	博士	013	密频模态波器的实现及其在智能结构中的应用	应用力学学报	001702	J
130	刘福强 张令弥	博士	013	作动器/传感器优化配置的研究进展	力学进展	003004	H
131	张令弥 刘福强	教授	013	Active Damping Enhancement of Flexible Intelligent Truss structures with Acceleration Measurements	PROC. Of the SPIE	2000	
132	刘福强 张令弥	博士	013	Model-Space Control of Flexible Intelligent Truss Structures Via Modal Filters	Proc. Of 18th International Modal Analysis Conference	2000	
133	刘福强 岳 林 张令弥	博士	013	基于模态滤波器的柔性智能桁架结构振动主动控制实验研究	航空学报	002106	H
134	周储伟 王鑫伟	博士后	013	Interfaqce damage analysis of fiber-Reinfor-ced composites	南京航空航天大学学报 (英文版)	001702	J
135	徐庆华 周传荣 罗志才	工程师	013	GPS 振动环境试验装置的研制	河海大学学报(自然科学版)	002806	H
136	苏鹤玲 赵向东 赵淳生	硕士	013	旋转驻波型超声电机摩擦界面的数学模型	南京航空航天大学第二届研究生学术会议	2000	
137	刘 剑 赵淳生	硕士	013	基于利用矩形板振动的直线型超声电机的设计	全国首届“振动与波的利用”学术会议	2000	

序号	姓名	职称	单位	论文题目	刊物、会议名称	年、卷、期	类别
138	熊克 陶宝祺 金江	副教授	013	形状记忆合金增强复合材料连接件模型的实验研究	实验力学	001502	J
139	熊克 陶宝祺 金江	副教授	013	Theoretical and Experimental Study on Shape Memory Alloy Torsion Actuator	国际航空科学大会 (ICAS2000)	2000	
140	夏文庆	讲师	014	蒸发制冷在机载冷却系统中的应用及热力循环分析	环控暨人机工效学术交流会	2000	
141	余莉		014	降落伞系统工作过程计算机仿技术初探	中国航空学会环控及人机工效学术会议	2000	
142	张大林 方贤德	讲师	014	加压供氧面罩呼气活门的呼气阻力数值计算	2000年环控暨人机工效学术交流会	2000	
143	王芳 郭宪民	副教授	014	提高热泵空调器冬季运行性能的措施	2000年环控暨人机工效学术交流会	2000	
144	张书贤 郭宪民 朱春玲	副教授	014	空调系统控制技术进展	2000年环控暨人机工效学术交流会	2000	
145	范铭 高鹰 葛海燕	讲师	014	竖壁膜状凝结理论分析	化工学报	005102	H*
146	葛海燕	讲师	014	竖壁膜状凝结扩展方程理论研究	江苏省制冷学会第四届年会	2000	

文章编号:1001-4888(2000)03-0441-07

复合材料层板构件气弹振动控制实验研究

陈勇¹, 陶宝祺¹, 高璠²

(1. 南京航空航天大学 智能材料与结构航空科技重点实验室, 南京 210016;

2. 东南大学 国家火电机组振动工程研究中心, 南京 210096)

摘要:飞机局部复合材料构件存在着因涡流作用诱发的弹性振动问题. 本文首先研究了表面粘贴型压电元件对复合材料构件的传感和驱动原理; 针对结构待控模态的要求, 采用了D-准则优化确定同位压电传感/驱动器在构件中的布置方案; 应用自适应振动前馈控制原理和方法, 构造了闭环控制系统; 分别利用正弦和方波信号激发气动声场, 对玻纤/环氧圆筒构件进行激振和振动控制实验; 结果表明: 构件主要待控模态的振动得到了有效抑制, 但也出现了高阶模态被激发的问题, 导致结构辐射噪声上升.

关键词:复合材料; 气动冲击; 振动抑制; 自适应控制; 智能

中图分类号: TB51; O324 **文献标识码:** A

1 引言

纤维增强复合材料具有优异的比强度、比刚度和可设计性, 在新型飞机中大量使用, 重量占飞机机翼、尾翼的20%~40%和直升机结构的40%~50%. 由于复合材料层板结构厚度方向缺少纤维增强, 对面外载荷、低能量冲击损伤及中面应力集中比较敏感, 因此, 在设计中必须考虑构件的动态特性和动态响应, 保证不发生因振动、噪声引起的性能退化及破坏.

设计规范^[1]一般采取储备频率设计原则, 目的是避开干扰频率的共振区, 减小构件的动态响应. 但在飞行中由于存在着宽频气动激励力, 很难保证构件的各阶模态完全避开激励频带, 因此局部复合材料构件会因弹性振动导致脱层失效. 如澳大利亚空军的F/A-18战斗机在大攻角飞行时, 因双尾垂之间形成强烈的涡流^[2], 导致脉动压力作用在垂尾的碳纤维/环氧壁板上, 产生很大的交变应力和复杂的位移响应, 显著降低了构件寿命. 目前, 一个重要的研究趋势就是针对结构待控模态的要求, 把压电元件作为复合材料的铺层, 采用主动控制技术对构件的振动进行抑制^[3].

• 收稿日期: 1999-09-10; 修订日期: 2000-08-03

基金项目: 国家自然科学基金、航空科学基金联合资助项目(59635140), 江苏省博士后科研基金资助项目

作者简介: 陈勇(1969—), 男, 讲师. 现为东南大学国家火电机组振动工程研究中心博士后. 研究方向为智能结构的振动控制、测控技术等.

为了实现对复合材料构件主要模态的振动抑制,必须解决传感器与驱动器的布局和控制律的设计问题.在本文的研究中,根据构件待控模态的控制要求,通过在复合材料构件表面粘贴压电传感器和驱动器,利用 D-优化准则确定传感器和驱动器的布置方案,采用自适应控制规律,构造了基于 PC 机和数据采集接口卡的闭环控制系统,对脉动气流激振下的玻纤/环氧构件进行振动主动控制实验,探索复合材料构件响应控制的基本原理和方法.

2 结构振动主动控制系统的设计原理

为了满足相容性要求,应把压电传感器和驱动器作为铺层埋入复合材料构件中.但由于制作工艺较为复杂,在本文的研究中采用了较为简便的表面粘贴工艺.

2.1 表面粘贴型压电元件的测量与驱动

在表面粘贴工艺中,机电耦合特性、粘结层及构件的物理性质都会影响压电传感器的输出.在图 1 所示的结构型式中,假设构件处于单向应力状态,为了减小横向效应,选择压电传感器的长宽比大于 8,此时传感器沿长度方向的应力近似均匀分布.不计边界效应的影响,则传感器所受的应力为

$$\sigma = -\frac{t_c}{t_b} Kch(\sqrt{\alpha} x) \sigma_1 + (1 - \frac{t_c}{t_b} \frac{\beta}{\alpha}) \sigma_1 \quad (1)$$

根据压电效应,传感器的等效电荷为

$$q = d_{31} A \sigma \quad (2)$$

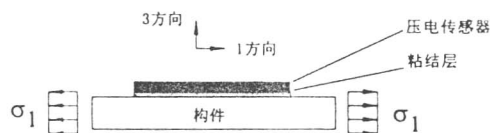


图 1 粘贴于结构表面的压电传感器

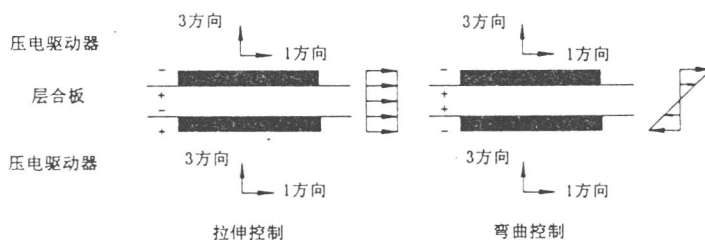


图 2 压电驱动器与复合材料的驱动模型

长方板型压电驱动器对称粘贴在复合材料构件表面,如图 2 所示.驱动器的变形取决于外加控制方式,在两压电驱动器的极化轴 3 方向施加同相控制电压,压电驱动器由逆压电效应产生 1 方向形变;形变受到粘结层和复合材料层板的约束,在粘结层及复合材料构件间产生拉/压应力或应变的传递.类似地,在两压电驱动器间施加反相控制电压,将产生可控弯曲应变.这种控制应变的耦合传递过程与压电驱动器、层合板及粘结层的机械性质有关^[4].当作用在压电驱动器上的同相控制电压为 V 时,传递到复合材料层板中面的驱动应变 ϵ'_x 为

$$\frac{\epsilon'_x(\bar{x})}{\Lambda} = \frac{6}{\phi_b + 6} - \frac{6}{(\phi_b + 6) \cosh(\Gamma \bar{x})} \cosh(\Gamma \bar{x}) \quad (3)$$

在以上各式中

$$\Gamma = \frac{\phi_s}{t_s^2} \left(\frac{\phi_b + 6}{\phi_b} \right), \quad \phi_b = \frac{E_s t_s b_b}{E_s t_s b_c}, \quad \phi_s = \frac{G_s t_s b_s}{E_s t_s b_c}, \quad \bar{t}_s = \frac{t_s}{l_c/2}, \quad \bar{x} = \frac{x}{l_c/2}, \quad \Lambda = \frac{d_{31} V}{t_c}$$

$$\alpha = \frac{E_{tb} + E_{tc}}{E_{ts} + E_{tc}} \frac{1}{E_{tb}} \frac{G}{t_s}, \quad \beta = \frac{E_{tc}}{E_{ts} + E_{tc}} \frac{G}{E_{ts}}, \quad K = \frac{-\beta}{\alpha \cosh(\sqrt{\alpha} L)}$$

E, G, t, b, l 分别表示杨氏、剪切弹性模量、厚度、宽度及长度,下标中的 b, s 和 c 分别表示层板、粘结层和压电陶瓷驱动器.

2.2 复合材料构件中压电元件网络的设计

在复合材料构件中,把压电传感器和驱动器对称地粘贴在同一位置的两侧表面,组成传感/驱动器对,实现对结构振动的同位控制.这种方式能使受控系统成为最小相位系统,保证了系统的稳定性,防止由于模态截断导致观测和控制溢出.

在确定构件中同位压电传感/驱动器的布置方案时,可采用以 Fisher 矩阵行列式最大化为目标函数的 D-优化方法^[5].在结构阻尼较小的条件下,该优化方法可以使传感器位置和控制输入问题与结构的模态频率解耦,只利用结构待控模态的振型信息就能最优地确定传感器的位置,使设计大为简化.

2.2.1 位置优化的数学模型

假设采用的压电传感/驱动器结构和尺寸均相同,每个传感器的输出都能统一地表达为

$$y_k = r_k^T \Phi p'(\eta)$$

$p'(\eta)$ 表示模态坐标 η 的 2 阶微分, r_k 是与传感器位置有关的向量.优化设计的目标函数为

$$S^*(m) = \max_{\beta} \sum_{i=1}^M \log \left[\sum_{k=1}^M \beta_k (r_k^T \varphi_i)^2 \right] \quad (5)$$

$$\text{s.t. } \beta \in B_m \quad B_m = \left[\beta: \sum_{k=1}^M \beta_k = m \right] \quad (6)$$

式中, N 为结构待控的模态数; M 为有限元模型中描述结构模态的维数; m 为布置的传感/驱动器对的数目, $m \leq M$; $r_k \in R^M$ 为第 k 个压电传感器的系数列向量; φ_i 为第 i 个待控模态的归一化振型矢量; β_k 为位置选择矩阵的元素,由 0 和 1 组成. $\beta_k = 1$, 表示结构对应网格处应包含一个同位传感/驱动器, $\beta_k = 0$ 则表示没有.

2.2.2 数学模型的优化求解

由式(5)可知:目标函数的实质是对压电传感器在各阶待控模态下输出信号的累计求和,设计变量 β 确定了传感器在有限元节点中的位置,约束条件是传感器的数量为 m .该优化过程是一个离散优化问题,可以采用随机试验法进行求解.求解过程如下:

1. 对复合材料构件的振动模态进行分析,确定待控的 N 个主要模态振型;
2. 根据控制器的设计规模(即约束条件)确定传感/驱动器对的数量 m ;
3. 令循环计数器 $j=1$,利用随机数发生器产生假设一个位置矩阵 β ,使其中 m 个元素为 1,其余为 0,得到各传感/驱动器对在结构中的一种布置方案,再由式(2)得到各个压电传感/驱动器的系数矩阵 r_k ;
4. 计算目标函数值 S ;
5. 重复步骤 3,将新的目标函数值与旧目标函数值相比较,记录下较大的目标函数值 S 及相应的位置矩阵 β ;
6. 若经过了一定次数的迭代后,即得到使目标函数较大的一种可行布置方案.

在有限元分析中,由于压电传感/驱动器的质量和尺寸与复合材料构件相比均较小,而且数量一般也较少,因此,为了简化分析过程,认为对构件质量、刚度矩阵的影响可以忽略不计.

2.3 基于自适应滤波的振动前馈控制器

在主动控制系统中,控制律设计是核心任务之一.基于自适应滤波的振动前馈控制^[6]能够以数字滤波器形式建立受控对象的数学模型,确定系统模型参数,采用递推公式计算最优控制器参数,控制驱动器的动作,使传感器处的受控响应与外扰响应相抵消,达到较高的控制品质.

基于自适应滤波的振动前馈控制系统如图3所示. d 为外扰激励下的无控输出, e 为有控输出, y 为自适应控制器的控制信号, H 是描述从驱动器到传感器之间的前控通道特性矩阵, W 为自适应控制器的权系数参数矩阵, X 为振动控制器的参考输入信号.

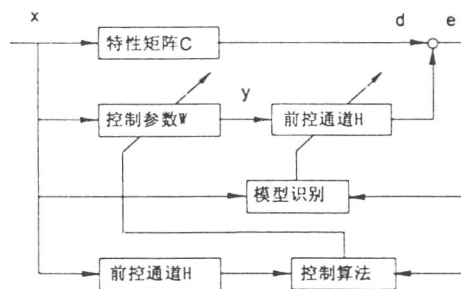


图3 基于自适应滤波的振动前馈控制原理图

若采用脉冲响应函数的描述形式,则 L 个传感通道, M 个控制通道的自适应振动前馈滤波—XLMS算法可以表示为

$$y(n) = X^T(n)W(n) \quad (7)$$

$$e(n) = d(n) + R^T(n)W \quad (8)$$

$$W(n+1) = W(n) - 2\mu e(n)R^T(n) \quad (9)$$

$$R(n) = [r_1(n), r_2(n), \dots, r_L(n)] \quad (10)$$

$$r_i(n) = [r_{i1}(n), r_{i1}(n-1), \dots, r_{i1}(n-I+1), \dots, r_{iM}(n), r_{iM}(n-1), \dots, r_{iM}(n-I+1)]^T \quad (11)$$

$$r_{in}(n-i) = \sum_{j=0}^{J-1} h_{nj}(n)x(n-j-i) \quad (12)$$

在本文的研究中,同位配置传感器与驱动器,即有 $L=M$.前向控制通道 H 原则上需要在线辨识,对计算机速度及算法的效率提出了很高的要求.但对多数结构而言,传输通道特性基本不变,并且可以用较低阶模型进行近似.因此,对控制对象预先进行离线识别和降阶,以简化控制器的设计^[6].离线识别时将外部激励源关闭,将可编程信号发生器信号输入控制通道,根据输入和输出数据进行控制通道的建模和降阶.

另外,为了简化控制器的设计,参考信号直接引自激励信号发生器;而将压电传感器的测量信号经电荷放大器和带通滤波器调理后作为自适应控制系统的误差信号.

3 复合材料构件振动控制的分析与实验

3.1 复合材料构件的有限元分析与压电元件布置

实验对象是一端封闭的复合材料圆筒构件,系正交各向异性的玻璃纤维/环氧层合板制成,直径 $\phi 1000\text{mm}$,高 520mm ,壁厚 5mm ,四点固定.为了估计结构的动态特性,采用SAP91对构件的振动模态进行计算,获得相应的振型数据.分析发现:(1)结构封闭端的低阶模态分别

是 25, 52, 86 和 126Hz; (2) 周向低阶模态分别为 79.7, 152.7, 215.4 和 252Hz; (3) 在 300~400Hz 的频率范围内, 构件的模态比较密集, 封闭端和圆筒径向模态存在耦合现象。

根据本系统中自适应控制器的设计规模, 确定传感驱动器的数量为 4 个。由于飞机涡流激励能量主要集中在 300~500Hz 较宽的频带, 而该圆筒的振动模态又大量集中在此范围内, 若考虑多个模态, 则会给传感器和驱动器的布置带来较大困难。因此, 只选择其中 380Hz 模态进行了优化, 结果如图 4 所示。

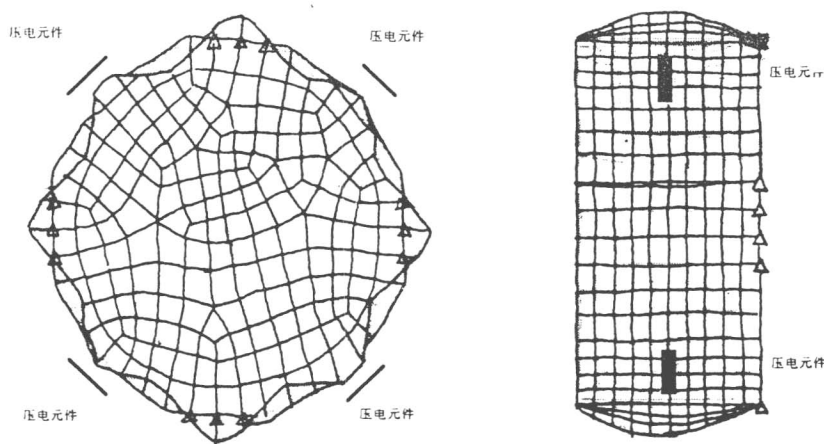


图 4 选择的圆筒构件振型及压电元件布置位置

3.2 实验方法与步骤

激励方式:

为了模拟作用在构件上的涡流激励力, 用 Goodwill GFG-813 信号发生器驱动扬声器, 采用不同频率成份的噪声场激励复合材料构件, 以激发筒壁的振动模态。粘贴在圆筒构件上的对位压电传感/驱动器尺寸 $40 \times 7 \times 1\text{mm}$, $d_{31} = 240 \times 10^{-12}\text{V/m}$, 长度方向沿圆筒构件的周向, 如图 4; 粘结剂为双组分快干环氧胶。

实验步骤:

1. 采用正弦信号输入扬声器, 利用其输出声场模拟气动冲击载荷激励复合材料圆筒构件, 压电传感器的信号经电荷放大器输出, 得到构件的动态响应信号;
2. 进行闭环控制试验, 将振动前馈控制器和控制信号由 D/A 输出, 再经 HS300 功率放大器驱动各个压电驱动器, 抑制结构的振动响应;
3. 对控制前后的结构响应进行频谱分析, 定量比较控制效果;
4. 再分别采用三角波和方波信号激励圆筒, 重复上述步骤, 比较不同激励频率成份下的控制效果, 分析基本规律。

3.3 典型实验结果与讨论

图 5 所示是 380Hz 的正弦和方波激励下, 控制前后结构响应功率谱密度的比较。正弦激励实验发现: 结构响应中包含了 50Hz 和 380Hz 两个分量, 控制后 380Hz 主激励频率的响应衰减了 6dB, 表明该模态的振动得到了明显的抑制, 但 50Hz 分量没有衰减, 另外, 在主频率得到

有效抑制的同时,构件的辐射噪声显著上升.

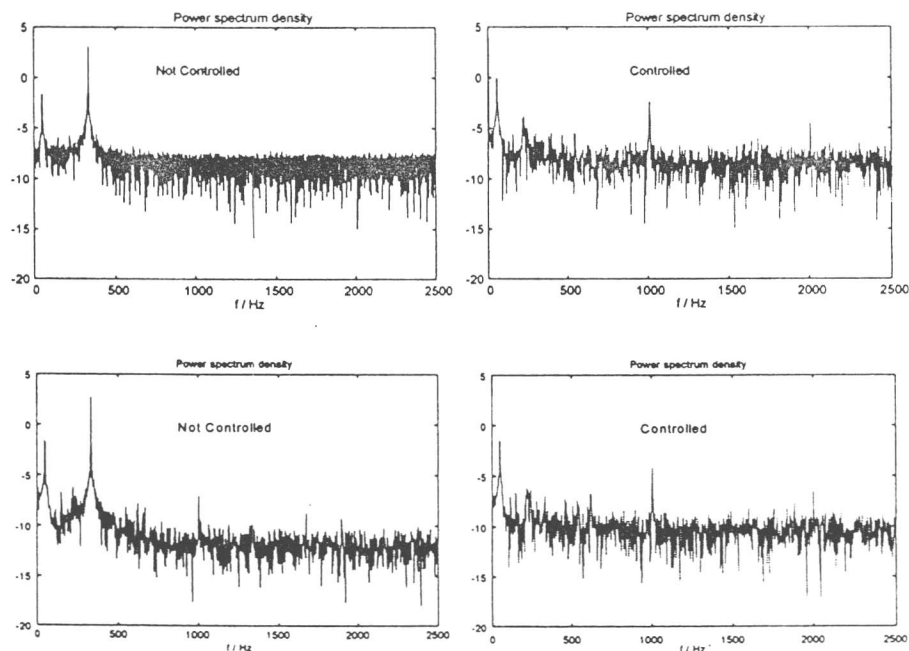


图 5 复合材料构件响应的功率谱密度

分析认为:① 50Hz 分量是由于控制电路中引入的电源干扰激励起端盖响应(52Hz 模态)造成的,由于驱动器只是针对径向模态的抑制而设计,因此对端盖的响应没有明显的控制效果.②辐射噪声水平的上升是由于数字控制器引入了高频成份,导致高阶模态被激发造成的.因为自适应控制器产生的数字信号通过 D/A 转换,在前后时序上相当于阶跃变化,引入的高频成份能激励起结构的高阶模态,导致结构响应中高阶成份上升.解决这个问题的途径之一是在 D/A 环节之后引入低通滤波器,滤除高频分量后再经功率放大器控制压电驱动器,但这会使控制通道特性产生一定变化,有待今后研究中进一步讨论.

从同频方波(50%占空比)激励的频谱分析中还发现,虽然 380Hz 分量得到了抑制,但其它模态的响应甚至加强,辐射噪声更为明显.

4 研究结论

本文通过在复合材料构件表面粘贴压电传感器和驱动器,采用自适应振动前馈方法对气动冲击载荷激励下的响应进行主动抑制,取得了较好效果.通过控制系统设计和实验结果的分析,得到如下结论:

(1) 针对复合材料构件待控模态的要求,采用 D-优化准则确定压电元件布置方案的原理和方法可行,复合材料构件的气动冲击响应得到了有效抑制.

(2) 在复合材料构件的振动控制实验中,对不同成份气动激励力进行了比较,结果表明:随着高频激励分量的增加,结构待控模态仍能得到有效抑制,但也造成了结构高阶模态被激发的问题,并导致结构辐射噪声的显著增加。

(3) 如何有效抑制因高频成份诱发的高阶模态振动有待进一步的深入研究。

参考文献:

- [1] 航空航天工业部科学技术研究院. 复合材料设计手册 [S]. 北京:航空工业出版社, 1990. 12—14.
- [2] Long Gordon. Future Directions in Aeronautical Composites [C/CD]. Proceedings of 21st Congress of the Council of the Aeronautical Sciences. Melbourne: International Council of the Aeronautical Sciences and the American Institute of Aeronautics and Astronautics, 1998.
- [3] Scott E Miller, Yaakov Osman, Haim Abramovich. Selective Modal Control of Anisotropic Piezo-laminated Shells via Self-Sensing Selective Modal Actuators [C]. Proceedings of 36rd Structure, Dynamic Mechanics Conference. Saint Diego: The American Institute of Aeronautics and Astronautics, 1995. 760—770.
- [4] 陈勇,陶宝棋,刘果. 柔性结构振动控制的初步分析与实验研究 [J]. 机械强度, 1998, 20(3):206—211.
- [5] Bayard D S, Hadaegh F Y, Meldrum D R. Optimization Experiment Design for Identification of Large Space Structures [J]. Automatica, 1988, 24(3):357—364.
- [6] 顾仲权,马扣根,陈卫东. 振动主动控制 [M]. 北京:国防工业出版社, 1997. 118—121.

An Experimental Study on Active Vibration Suppression of Composite Structures

CHEN Yong¹, TAO Bao-qi¹, GAO Wei²

(1. The Aeronautical Lab for Smart Materials and Structures, NUAA, 210016; 2. National Research Center of Turbo Engine Vibration, South East University, Nanjing 210016)

Abstract: The vortex-induced buffeting loads on aircraft may cause high cyclic strain and stress in aircraft composite structure and lead to composite delamination. To simulate the active vibration suppression for such composite structures, an experimental system is designed, where collocated piezoelectric sensors/actuators are bonded to the surface of a composite cylindrical shell, and the maximum determinant of Fisher Information Matrix criteria is used to arrange the piezoelectric network. With sine and square acoustic fields as exciting source and with the filtered adaptive control algorithm to control the deformation of the actuators, a close loop control is established to minimize the selected vibration modes of the cylindrical shell. Experiments on the system show that the selected modes can be suppressed effectively but higher modes are also excited and lead to significant noise radiation which should be treated carefully in future research.

Key Words: composite material; aero-elastic buffeting; vibration suppression; adaptive control; smart structure

Article ID: 1000-9361(2000)04-0198-06

ANALYSIS OF AN ELECTROSTRICTIVE STACK ACTUATOR FOR ACTIVE TRAILING EDGE FLAPS

CHEN Yong(陈 勇)¹, GAO Wei(高 甾)², GU Zhong-quan(顾仲权)³, TAO Bao-qi(陶宝祺)¹

(1. *Aeronautical Lab for Smart Materials and Structures, Nanjing University of Aeronautics and Astronautics, Nanjing 210016, China*)

(2. *National Research Center of Generator Vibration, Southeast University, Nanjing 210096, China*)

(3. *National Lab for Rotorcraft Dynamics, Nanjing University of Aeronautics and Astronautics, Nanjing 210016, China*)

Abstract: Stack actuator is a solid-state driving component of Active Tailing Edge Flap in smart rotor systems. It is a multi-layer serial structure of basic units composed of electrostrictive and adhesive layers. In this paper, a dynamic model of the actuator is derived based on the constitutive equation of electrostrictive material and the equation of motion. Theoretical analysis is made on the factors involved in the design of the actuator, which reveals that the electrostrictive layer and the adhesive layer should be optimized to compromise between displacement and frequency requirements. In the final part of the paper, the experiment of an ATEF system is introduced. The results show that the model is reasonable. It also suggests that the bending stiffness of elastic mechanism is an important factor in design, which should be carefully studied to provide satisfactory dynamic response of the ATEF system.

Key words: adaptive rotor; stack actuator; electrostrictive material

CLC number: V214 **Document code:** A

Helicopter is a complex dynamic system with many rotating components. The rotor blades operate in a highly complex aerodynamic environment. The vibratory hub load, which is caused by cyclic variation of centrifugal and aerodynamic load of the rotating blades in flight, is transmitted to the fuselage, resulting in serious vibration and noise of the structure. It is one of the most important exciting sources in helicopters.

There has long been a desire to reduce helicopter vibration and to improve its performance. Control schemes adopted so far can be classified as either passive or active control technologies. The passive technologies include optimization of rotor hub, blade and the fuselage, hub or blade mounted passive vibration absorbers and anti-resonant vibra-

tion isolators. One of the major disadvantages with passive technologies is that they are designed to provide maximum vibration reduction at a specific frequency; therefore, their performance is degraded significantly with changes in the operating conditions of the rotor system.

With the development of computer science and active control technology, increasing efforts have been devoted to active control technologies to benefit helicopter vibration suppression in recent years. Earlier studies include Higher Harmonic Control (HHC)^[1] and Individual Blade Control (IBC)^[2], which is aimed to reduce the vibratory blade load by oscillating the blade in pitch motion using hydraulic actuators. It is successful in suppressing the vibration of the fuselage; however, its

Received date: 2000-04-21; Revision received date: 2000-08-22

Foundation Item: Chinese Natural Science Foundation(59635140 and 59875035)

Article URL: <http://www.hkxb.net.cn/cja/2000/04/0198/>

application is limited by serious energy consumption.

To overcome these difficulties, a new concept in helicopter vibration control is the smart rotor system. In this scheme, actuators are embedded in composite blades. They are used to activate the trailing edge flaps in higher harmonic pitch motion to adjust the lift force actively. Under the regulation of a control system, the vibratory hub load can be counteracted actively at the source.

Compared with the HHC and IBC concept, the smart rotor is promising in reducing energy consumption and simplifying the control system^[3]. However, in order to satisfy the requirements of vibratory load control, the flaps have to be controlled both quickly and precisely (frequency response up to 4ω , amplitude of pitch angle between 6° to 8° ^[4,5]). Currently, many experimental studies are being taken to develop ATEF systems using integrated actuator technology in smart structure, and to satisfy both the compact and high efficiency requirements.

The integrated actuators are made of functional materials, producing displacement under external voltage. Electrostrictive material is a kind of ferroelectric ceramic, the strain is approximately of the 2nd order relationship with actuating electric field, and can be used in the development of a solid actuator in smart rotor systems. However, since the displacement of the actuator not only depends on its structure, but also relies on external force and voltage, a mathematical model is needed to predict its output characteristics in design.

In this paper, a dynamic model of the stack actuator is derived using the principle of force equivalence, which is based on the constitutive equation of ferroelectric material and the equation of motion. Theoretical analysis is made on the factors involved in the design of stack actuators. At the end of the paper, a stack actuator is designed according to theoretical analysis. Experiments of an adaptive trailing edge flap model are introduced to verify the feasibility of the model.

1 Mechanical Model of Stack Actuator

1.1 Structural analysis of stack actuator

A driving mechanism of ATEF is shown in Fig. 1. The displacement of the actuator is determined by the structure, electric-mechanical conversion efficiency of functional material, external load and frequency. Since the displacement is relatively small, it is amplified by an L-shaped elastic lever mechanism before driving the trailing edge flap through a plane rocker mechanism. Besides displacement amplification, the elastic mechanism is also used to overcome the clearance between mechanical joints.

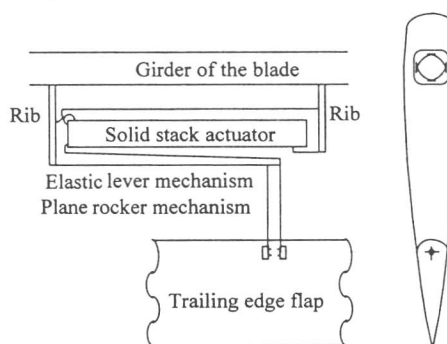


Fig. 1 Schematic diagram of ATEF system

To increase the displacement and to avoid decrease in load capacity, a stack structure is adopted in actuator design. A serial multi-layer stack structure of basic units is the design of actuators, which is composed of an electrostrictive layer, electrode layer and adhesive layer, as shown in Fig. 2.

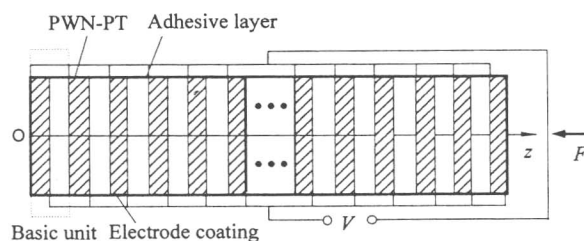


Fig. 2 Structure of stack actuator

Without taking the boundary effect and current leak into account, displacement occurs to the stack actuator under electric field in the direction of thickness (polarization).

Since the electrode coating is so thin in thickness that it can be neglected in analysis. Every basic unit is composed of two parts; the electrostrictive

tive layer and the adhesive layer. The whole actuator is a serial system made up of many identical basic units.

1.2 Mechanical model of electrostrictive layer

The electrostrictive material is a kind of ferroelectric ceramics with non-linear mechanical and electrical coupling relationship, and there is a linear piezoelectric term and a second order of electrostrictive term in the constitutive equation. Under the combined action of force and electric field, its mechanical and electrical coupling relationship can be expressed as^[6]

$$S_3 = s_{3i}^E T_i + (g_{mi} + Q_{mr3} D_r) / D_m \quad (1)$$

where S_3 , T_i and D_m are strain in Z direction, stress and electric potential; s_{ij}^E , g_{mi} and Q_{mr3} are flexibility coefficient, piezoelectric voltage constant and electrostrictive coefficient of the ferroelectric material respectively. As for the electrostrictive material, the working temperature is often slightly higher than its Curie point; there is no piezoelectric effect while the electrostrictive effect is strong, and only the second term is taken into consideration.

In a serial structure, the electrostrictive layer only bears axial load F in the direction of thickness. Defining the density of electrostrictive material as ρ , displacement in Z direction as u_3 , according to Newton's second law and $S_3 = \partial u_3 / \partial z$, the equation of motion can be derived as follows in z direction^[4].

$$\rho \frac{\partial^2 u_3}{\partial t^2} = \frac{1}{s_{33}^E} \frac{\partial^2 u_3}{\partial z^2} \quad (2)$$

Supposing $V = \sin \omega t$ and neglecting the boundary effect, the stable displacement of the electrostrictive layer can be expressed as

$$u_3 = \frac{\delta \sin(\omega z / v_3^E)}{\sin(\omega l / v_3^E)} e^{j\omega t}, \quad v_3^E = \left(\frac{1}{\rho s_{33}^E} \right)^{1/2} \quad (3)$$

By substituting the relationship between strain and displacement into Eqs. (1) and (3), then

$$\delta = \frac{v_3^E \sin \frac{\omega l}{v_3^E} (s_{33}^E T_3 + g_{33} D_3 + Q_{333} D_3^2)}{\omega e^{j\omega t} \cos \frac{\omega z}{v_3^E}} \quad (4)$$

Considering the axial load F is evenly distributed on the cross-section, Eq. (4) can be

rewritten as

$$\delta|_{z=l} = \frac{v_3^E \sin \frac{\omega l}{v_3^E} \left(s_{33}^E \frac{F}{A} + g_{33} D_3 + Q_{333} D_3^2 \right)}{\omega e^{j\omega t} \cos \frac{\omega l}{v_3^E}} \quad (5)$$

It should be noticed that there is a hysteresis effect between potential displacement and the controlled field in electrostrictive material under cyclic electric field. Without considering this process, the displacement of the electrostrictive layer can be expressed as

$$\delta = \frac{F + g_{33} \epsilon_{33} \left(\frac{V_3}{l s_{33}^E} \right) + \frac{\epsilon_{33}^2 Q_{333} A V_3^2}{l^2 s_{33}^E}}{K_F} = \frac{F + F(V)}{K_F} \quad (6)$$

$$K_e = \frac{v_3^E \sin \frac{\omega l}{v_3^E}}{\omega \cos \frac{\omega l}{v_3^E}}, \quad K_F = \frac{A}{K_e s_{33}^E}$$

$$F(V) = g_{33} \epsilon_{33} \frac{V_3}{l s_{33}^E} + \frac{\epsilon_{33}^2 Q_{333} A V_3^2}{l^2 s_{33}^E} \quad (7)$$

where ϵ_{33} , l , A represent the dielectric coefficient, thickness of electrostrictive layer and the cross-sectional area of the actuator. According to Eqs. (6) and (7), the electrostrictive layer is equivalent to a parallel system of a spring whose dynamic stiffness is K_F and a force source $F(V)$. The stiffness- K_F depends on the cross-sectional area, thickness, density, flexibility coefficient of the electrostrictive layer and frequency, respectively, while the force source is determined by the area, voltage and electrostrictive coefficient of electrostrictive material. One point to be noted is that the dielectric coefficient of electrostrictive material is a non-linear function of external load and electric field, which increases with the density of electric field and decreases with frequency. One may conclude that the force and displacement of the electrostrictive layer in stack actuators are in non-linear relationship with frequency, and closely related to external load.

1.3 Mechanical model of basic element

Neglecting the damping, the mechanical model of the adhesive layer can be treated as a mass-

spring system. M is the concentrated mass of the adhesive layer; K_m is stiffness of the spring; E , A and t are the elastic modulus, cross-sectional area and thickness of the adhesive layer, respectively.

$$K_m = \frac{EA}{t} \quad (8)$$

According to Eqs. (6) and (8), the basic unit of the stack actuator can be shown as Fig. 3.

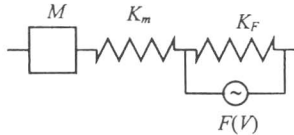


Fig. 3 Mechanical model of the basic unit

1.4 Mechanical model of stack actuator

Since the stack actuator is a multi-layer serial structure of basic units, it is equivalent to a serial structure in mechanics, and a parallel system in electricity, as shown in Fig. 4.

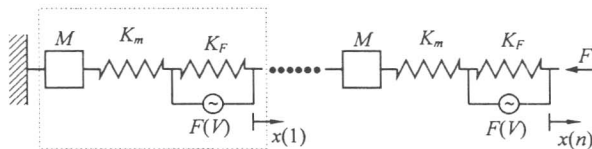


Fig. 4 Mechanical model of the stack actuator

2 Design and Analysis of Stack Actuators

In order to counteract the $n\omega$ harmonic components in lift force of rotor systems by adjusting the position of ATEF, the stack actuator has to produce large displacement at high frequency.

The serial structure of stack actuators is beneficial in increasing displacement; however, the first mode frequency is also decreased significantly. The adhesive layer is an important factor in design because its high elastic modulus and small thickness can help to increase equivalent stiffness, decrease equivalent mass and to increase the frequency of the first mode. In the design of the electrostrictive layer, the displacement can be improved by a decrease in thickness; however, it may also lead to non-linearity and hysteresis in displacement, which should be compensated for in application.

It follows that an optimization method can be used to determine the dimensions of the stack actuator, satisfying both displacement and frequency

requirements of smart rotors at the same time.

3 Experiments of Stack Actuator and ATEF Model

A solid stack actuator is designed based on the above analysis, as shown in Table 1. Experiments and analysis are made to verify the feasibility of the derived mechanical models. The electrostrictive material is PWN-PT, which was provided by Shanghai Institute of Ceramics, Chinese Academy of Sciences^[7]. Annealing technique is used to reduce the hysteresis effect and loss.

Table 1 Dimension of Stack Actuator

Functional Material	PMN-PT	Cross-section	9mm×9mm
Thickness of Electrostrictive Layer	0.3mm	Thickness of Adhesive Layer	0.1mm
Length of Actuator	135mm	Lag	6.4%
Block force	800N	Maximum Displacement	90μm

3.1 Displacement of the stack actuator

In experiments, the laser reflection method is used to measure the displacement of the stack actuator. The results are compared with simulation data, as shown in Fig. 5. It is found that there are

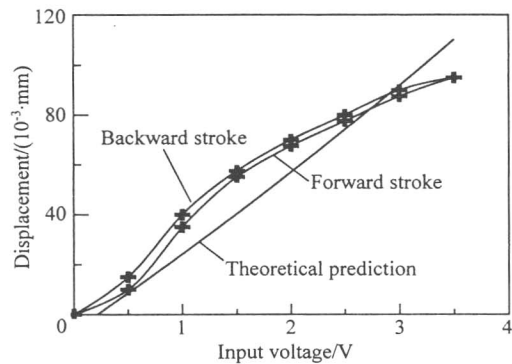


Fig. 5 Displacement of stack actuator

significant hysteresis and non-linearity in experiment, and the simulation result is reasonable in expressing the displacement of the actuator. According to the analysis, the reason for the error is the hysteresis effect in phase transition process of electrostrictive material, in which the physical performance is changed significantly. However, those parameters, such as the dielectric and electrostrictive coefficients, are treated as constants in simulation. Experimental results also suggest that a com-

pensation method is needed to improve the non-linearity in future close loop ATEF model experiments.

3.2 Response of the ATEF model

Fig. 6 is the response of ATEF model without rotating and external load. It can be found that the maximum deflection of flap is up to 9.8 degrees in static test under 400V-voltage. However, frequency response of the ATEF model is as low as 10 Hz. Further increase in frequency will lead to noticeable non-linearity in deflection of the flap, which is far from expected in the theoretical model.

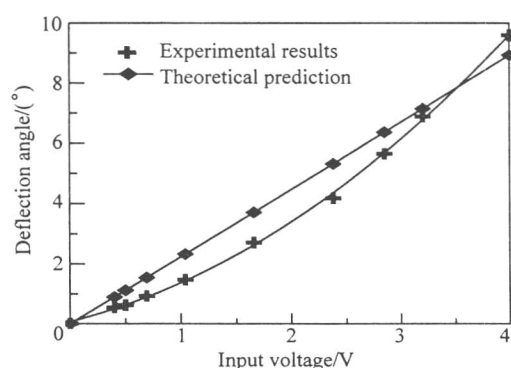


Fig. 6(a) Deflection curve of ATEF model

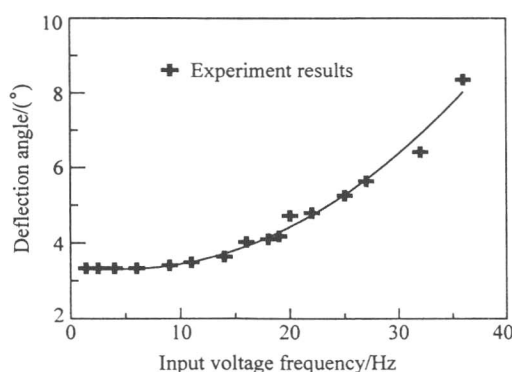


Fig. 6(b) Frequency response of ATEF model

According to the analysis, the non-linearity in deflection of the ATEF model is caused by the hysteresis and non-linearity in the displacement of the stack actuator. On the other hand, the plane rocker mechanism can not be treated as a linear system when the deflection is large. This means that a suitable compensation method is needed by adjusting the voltage on the actuator to improve its displacement characteristics.

Dynamic analysis is made on the ATEF mod-

el. Modal analysis of the elastic mechanism shows that the frequency of the first mode is 102 Hz, which is far above the required frequency of ATEF, and the corresponding mode shape is bending in the direction of displacement. Further finite element simulation reveals that there is a deformation under the combined action of inertia force, aerodynamic force and centrifugal force, which leads to non-linearity in the response of the ATEF model. The reason for the deformation is that the bending stiffness of the elastic mechanism is too weak. Simulation also demonstrates that although the response of the ATEF model can be significantly improved by increase in the stiffness of the elastic mechanism, however, the deflection angle will be decreased at the same time.

This implies that apart from the stack actuator, the elastic mechanism is an equally important factor to be considered in the design of ATEF model. Since there is a contradiction between the deflection angle and the frequency response in the bending stiffness of the elastic mechanism, an optimization method can be applied to balance both requirements, utilizing the huge force of the stack actuator.

4 Conclusions

In this paper, a theoretical model of the stack actuator is derived. Conclusions can be drawn from analysis of the factors involved in design and the experiments of the ATEF model.

(1) The electrostrictive layer is equivalent to a parallel system of spring and force. The adhesive layer can be treated as a spring-mass system. The stack actuator becomes a serial system of basic units in mechanics and a parallel system in electricity.

(2) The serial structure of the stack actuator is beneficial in increasing displacement. However, it can lead to a decrease in frequency response. The adhesive layer is an important factor in the design of actuators because larger elastic modulus and smaller thickness of the layer can improve the frequency of the actuator. It can increase the dis-